IOPscience iopscience.iop.org

Home Search Collections Journals About Contact us My IOPscience

Relaxation-stimulated resonances in Mössbauer absorption spectra under radiofrequency magnetic field excitation

This article has been downloaded from IOPscience. Please scroll down to see the full text article.

2000 J. Phys.: Condens. Matter 12 623

(http://iopscience.iop.org/0953-8984/12/5/310)

View the table of contents for this issue, or go to the journal homepage for more

Download details:
IP Address: 171.66.16.218
The article was downloaded on 15/05/2010 at 19:40

Please note that terms and conditions apply.

J. Phys.: Condens. Matter **12** (2000) 623–635. Printed in the UK PII: S0953-8984(00)05386-8

Relaxation-stimulated resonances in Mössbauer absorption spectra under radiofrequency magnetic field excitation

A M Afanas'ev†, M A Chuev† and J Hesse‡

† Institute of Physics and Technology, Russian Academy of Sciences, Nakhimovskii Avenue 36, 117218 Moscow, Russia

‡ Institut für Metallphysik und Nukleare Festkörperphysik, Technische Universität Braunschweig, Mendelssohnstrasse 3, D-38106 Braunschweig, Germany

Received 22 June 1999, in final form 20 September 1999

Abstract. A new type of resonant phenomena in the Mössbauer spectroscopy of soft magnetic materials in radiofrequency (rf) magnetic fields is predicted for the rf field frequencies related to those of components of the magnetic hyperfine structure via the parametric resonance condition. Resonant effects of this kind are still unknown in physics; they are realized not at frequencies of transitions between the energy sub-levels of the ground or excited nuclear states, which take place in conventional nuclear magnetic resonance, but at frequencies which are a combination of the frequencies of hyperfine transitions. In this case a separation between the real energy levels can exceed the value of the 'resonant' frequency by about 10 orders of magnitude and the resonant rf field sets as if in coherency between these energy levels. Such resonances can only be observed when relaxation processes play an essential role, which permits them to be defined as the relaxation-stimulated resonances. The simplest relaxation model of so-called one-way and localized relaxation is proposed. Within this model an analytical expression for Mössbauer absorption spectra is derived, based on which the specific features of the new resonant effects are analysed in detail.

1. Introduction

Studies of the Mössbauer spectra of magnetic materials under external radiofrequency (rf) magnetic field excitation are of interest mainly in connection with the collapse effect found by Pfeiffer in 1971 [1]. When a strong enough rf field is applied, a well-resolved magnetic hyperfine (HF) structure collapses into a single central line (or quadrupole doublet) accompanied with sidebands. This effect has been observed for a number of soft magnetic materials (see [2] and references therein). One more range of phenomena in the field is associated with the observation of double gamma-magnetic resonance [3]. At the rf field frequency, ω_{rf}, equal to one of the nuclear magnetic resonance frequencies for ground (ω_g) or excited (ω_e) nuclear states, the strongest influence of the rf field on the shape of Mössbauer absorption spectra is expected. Therefore, in this case a splitting of all spectral components is predicted. Attempts to observe the effect started in the 1960s [3], but they were ineffective for a long time, until recently, when the nuclear magnetic resonance at the excited ^{57}Fe nuclear level was observed by Kazan physicists (see [4] and references therein).

In the present paper, resonant phenomena of a qualitatively new type are predicted. The new resonances should reveal themselves in the spectra taken at the parametric resonance condition, i.e. at

$$\omega_{rf} = \frac{2|M\omega_e - m\omega_g|}{n} \tag{1}$$

0953-8984/00/050623+13$30.00 © 2000 IOP Publishing Ltd

where n is an integer, m and M are the projections of nuclear spin in the ground and excited states, respectively, on the direction of the hyperfine field at the nucleus. Resonant effects of this kind are still unknown and their non-trivial character becomes evident if one recalls that the energy separation between the ground and excited nuclear levels is larger than the splitting of the nuclear levels in a hyperfine field by about 10 orders of magnitude. In spite of this, the resonant rf field sets as if in coherency between the hyperfine sub-levels of the nucleus in the ground and excited states. These resonant effects can be observed only when relaxation processes play an essential role in the sample's magnetization reversal. For this very reason, resonances of the kind (1) will be called *relaxation-stimulated resonances*.

A theory developed in [5] for the description of relaxation Mössbauer absorption spectra under rf magnetic field excitation allows one to calculate the spectra as a function of the rf field frequency and amplitude and by that, naturally, to elucidate the question of the presence of new resonances. Simply by means of numerical calculations based on the general equations, these new resonances have been found. However, owing to the singularity of these phenomena, here we simplify the very relaxation model to such an extent that permits the final equations for the absorption spectrum to be derived in a relatively simple form. Along with that, in section 2, we introduce a model of *one-way and localized relaxation* (OWLR), a special type of relaxation process.

In section 3, an analytical expression for the description of Mössbauer absorption spectra within the OWLR model is derived. This expression allows one to describe completely the collapse effect and to carry out a simple analysis of the relaxation-stimulated resonances as a function of relaxation parameters. The latter is described in section 4.

2. Model of OWLR

Consider a sample as an ensemble of single-domain ferromagnetic particles with unidirectional magnetic anisotropy energy of which E_{an} is assumed to be large enough so that

$$E_{an} = KV \gg k_B T \tag{2}$$

where V is the volume of the particle, K is the magnetic anisotropy constant, T is the temperature, and k_B is the Boltzmann constant. Owing to condition (2), it is supposed that, in the absence of an external magnetic field, each particle can stay in only two states, 1 and 2, with the same energy and opposite directions of the particle's magnetic moment along the easiest magnetization axis. Generally speaking, these states are bound with each other through relaxation processes described by the probabilities of the transitions per unit of time, p_{12} and p_{21}, which are equal to each other with no external magnetic field. When an external magnetic field is applied, the energies of these states become different and their magnetic moments change in direction in order to tune to the direction of the magnetic field. Moreover, the probabilities of the transitions, p_{12} and p_{21}, become different so that in accordance with the detailed balancing principle, the transition from the upper to the lower level appears to be more probable than the opposite transition (see figure 1). This difference is determined by various energy barriers, U_1 and U_2, to be overcome for the downward and upward transitions.

In an external rf magnetic field

$$H(t) = H_0 \cos \omega_{rf} t \tag{3}$$

the relaxation rates can be represented in the form

$$\begin{aligned} p_{12}(t) &= p_0 \exp[-U_1(t)/k_B T] \\ p_{21}(t) &= p_0 \exp[-U_2(t)/k_B T] \end{aligned} \tag{4}$$

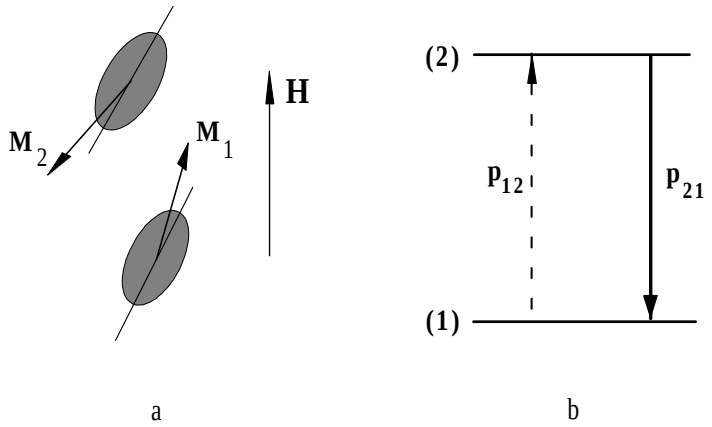

Figure 1. Two equilibrium states of a particle with different directions of its magnetic moment $\boldsymbol{M}$ in an external magnetic field $\boldsymbol{H}$ (a) and a scheme of the transitions between the states (b).

where p_0 is a constant slightly dependent on the magnetic field strength $H(t)$. The values of the energy barriers for single-domain particles with different orientation of the easiest magnetization axis have long since been obtained by Stoner and Wohlfarth [6]. According to the results of this work, one can find that for a particle with the easiest magnetization axis parallel to the direction of the magnetic field

$$U_{1,2}(t) = 2KV\frac{[H_c \pm |H(t)|]^2}{H_c^2} \tag{5}$$

where $H_c = 2K/M_0$ is the so-called critical field and M_0 is the specific magnetization of the particle. Equation (5) applies at the field strength $H(t) < H_c$, while at $H(t) > H_c$, according to [6], the value of $U_2(t)$ is equal to zero and $U_1(t)$ assumes the value of $2M_0H(t)$.

From equations (2), (4) and (5), one can neglect relaxation processes in the absence of a magnetic field. When a magnetic field is applied, the relaxation process remains activated, but there are different energy barriers for the downward and upward transitions. The energy barrier for the upward transition increases with increasing field strength and, hence, such transitions can also be disregarded. On the other hand, for the downward transition, the energy barrier U_2 decreases with increasing field strength and when the field strength reaches a certain value, the relaxation processes become so intense that they influence the shape of the Mössbauer spectra. Relaxation processes of this kind, when only the downward transitions can be taken into account and the upward transitions can be neglected, will be referred to as *one-way relaxation*.

As seen from equation (5), intense relaxation processes will occur at maximum values of the field strength, i.e. at moments

$$t_k = kT_{rf}/2 \tag{6}$$

where k is an integer and $T_{rf} = 2\pi/\omega_{rf}$ is the rf field period. Therefore, at high KV the relaxation processes should be taken into consideration only in the time intervals ($t_k - t_\varepsilon$, $t_k + t_\varepsilon$), where t_ε is much smaller than T_{rf}. We introduce the integral characteristics of the relaxation process, r and q, defined by

$$r = \exp\left[-2\int_{T_{rf}/2-t_\varepsilon}^{T_{rf}/2} p_{21}(t)\,\mathrm{d}t\right]$$
$$q = 1 - r. \tag{7}$$

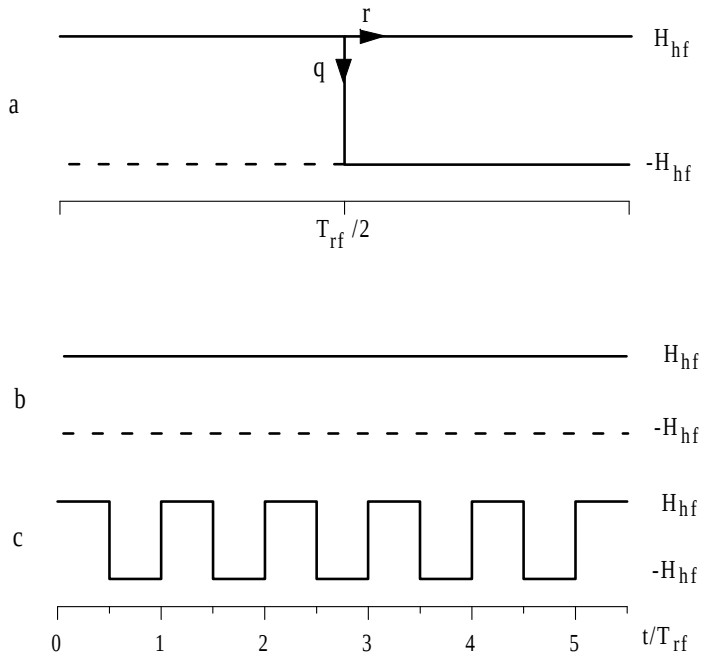

Figure 2. Time trajectories of the hyperfine magnetic field in the model of OWLR (a), with no relaxation at $q = 0$ (b), and in the regime of the complete particle's magnetization reversal at $q = 1$ (c).

Here r determines the probability of a particle staying in the same state on passing the point t_k and q is the probability that it changes its state on passing this point. As one can see below, just these integral characteristics will determine the shape of the Mössbauer spectra.

Now we can introduce a model of so-called *localized relaxation* where the relaxation is considered to take place in an infinitely small time interval, around t_k, so that the resulting effect of the relaxation can be completely described by the parameters r and q. Due to the exponential $p_{21}(t)$ dependence (4), one can extend the time interval t_ε in equation (7) up to $T_{rf}/4$ with an exponential accuracy, which results in

$$r = \exp\left[-2\int_{T_{rf}/4}^{T_{rf}/2} p_{21}(t)\,\mathrm{d}t\right]. \tag{8}$$

Note that within this model the time trajectories of the hyperfine field become stochastic in character, as shown in figure 2, and in a moment t_k there occurs a bifurcation of the trajectories; one of them remains in the same direction of the hyperfine field and the other changes to the opposite direction. As seen from the figure, the time trajectories for $q = 0$ and $q = 1$ are deterministic in character. The first case with $q = 0$ is trivial and corresponds to the time-independent hyperfine field, while the second case has a simple analytical solution which describes the collapse effect and the formation of sidebands [7, 8].

The relaxation model considered above is the simplest one and can be described by parameter r or q which can represent different physical processes, for instance, the presence of the interparticle interaction or its absence. On the other hand, as one can see below, within this model a rather simple analytical expression for the description of the Mössbauer absorption spectra can be derived so that qualitative effects of a rf magnetic field can be traced.

3. Mössbauer absorption spectra within the model of OWLR

A theory on the relaxation Mössbauer spectra of single-domain ferromagnetic particles under rf magnetic field excitation was first developed in [5] under the assumption that changes in the direction of the particle's magnetic moment can be neglected and the hyperfine field at nucleus H_{hf} can change only to the opposite direction as a result of relaxation processes. According to the results of this work, we have for the absorption cross-section

$$\sigma(\omega) = \frac{\sigma_a \Gamma_0^2}{4} \sum_{\alpha} |C_\alpha|^2 \varphi_\alpha(\omega) \tag{9}$$

where $\alpha \equiv (M,\ m)$, the coefficients C_α determine the intensities of the corresponding hyperfine transitions and can be expressed in terms of the Clebsch–Gordan coefficients, σ_a is the effective absorber thickness, Γ_0 is the width of the excited nuclear level, and

$$\varphi_\alpha(\omega) = \frac{1}{\Gamma_0 T_{rf}} \int_0^{T_{rf}} \mathrm{d}t \int_t^{t+T_{rf}} \mathrm{d}t' \langle W(t)| \frac{\mathrm{e}^{\mathrm{i}\tilde{\omega}(t'-t)}}{\hat{1} - \mathrm{e}^{\mathrm{i}\tilde{\omega}T_{rf}} \hat{G}_\alpha(t, t+T_{rf})} \hat{G}_\alpha(t, t')|1\rangle + \text{c.c.} \tag{10}$$

Here $\tilde{\omega} = \omega + \mathrm{i}\Gamma_0/2$,

$$\hat{G}_\alpha(t, t') = \hat{T} \exp\left[\int_t^{t'} \mathrm{d}t''(-\mathrm{i}\hat{\omega}_\alpha - \hat{P}(t'')) \right] \tag{11}$$

$$\hat{P}(t) = \begin{pmatrix} p_{12}(t) & -p_{12}(t) \\ -p_{21}(t) & p_{21}(t) \end{pmatrix} \tag{12}$$

$$\hat{\omega}_\alpha = \begin{pmatrix} \omega_\alpha & 0 \\ 0 & -\omega_\alpha \end{pmatrix} \tag{13}$$

where $\hat{T}$ is the time-ordering operator, $\omega_\alpha = M\omega_e - m\omega_g$, $\omega_{e,g} = g_{e,g}\mu_N H_{hf}$, μ_N is the nuclear magneton, $g_{g,e}$ are the nuclear g-factors for the ground and excited nuclear states, respectively, and the vector of population of the energy states, $\langle W(t)|$, is completely defined by the relaxation process

$$\frac{\mathrm{d}\langle W(t)|}{\mathrm{d}t} = -\langle W(t)|\hat{P}(t). \tag{14}$$

In solving this equation one should use the periodicity condition instead of the initial condition

$$\langle W(t + T_{rf})| = \langle W(t)|. \tag{15}$$

So, for the OLWR model discussed in the previous section one can easily obtain

$$\langle W(t)| = \begin{cases} \langle W_1| = \dfrac{1}{1+r}(1\ r) & \text{for } t \in (t_{2k}, t_{2k+1}) \\ \langle W_2| = \dfrac{1}{1+r}(r\ 1) & \text{for } t \in (t_{2k+1}, t_{2k+2}). \end{cases} \tag{16}$$

Using equations (9)–(15) one can calculate the Mössbauer absorption spectra for arbitrary amplitude and frequency of a rf field with no restrictions on the character of the relaxation processes. Since the operators $\hat{\omega}_\alpha$ and $\hat{P}$ do not commute with each other and the operators $\hat{P}(t)$ in the general case do not commute in different moments, it is necessary to perform relatively complicated calculations, a major part being the calculations of the chronological ordering operators. The power of the modern computer allows one to carry out much more complicated calculations in comparison with those in the case considered here (see, for instance, [8]). However, there is no possibility of a qualitative analysis of the transformation of the Mössbauer spectra. The simplified OWLR model just removes this defect.

Indeed, in the OWLR model, between the points of localization of the relaxation processes, one can neglect the relaxation and a simple expression for the Green function, $\hat{G}_\alpha(t,t')$, is obtained

$$\hat{G}_\alpha(t,t') = \begin{pmatrix} \mathrm{e}^{-\mathrm{i}\omega_\alpha(t'-t)} & 0 \\ 0 & \mathrm{e}^{\mathrm{i}\omega_\alpha(t'-t)} \end{pmatrix} \qquad \text{for } (t,t') \in (t_k, t_{k+1}). \tag{17}$$

In calculating the functions $\hat{G}_\alpha(t,t')$ in the vicinity of the points t_k one can neglect terms of the hyperfine interactions and retain only the relaxation operator $\hat{P}$. Moreover, in our model of the one-way relaxation the operators $\hat{P}(t)$ do commute in different moments, which allows the corresponding functions $\hat{G}_\alpha(t,t')$ to be expressed in terms of the integral relaxation characteristics r and q (see equation (8)):

$$\hat{G}_\alpha(t,t') = \hat{R}_1 = \begin{pmatrix} r & r \\ 0 & 1 \end{pmatrix} \qquad \text{for } t \in (t_{2k+1} - t_\varepsilon, t_{2k+1}),\ t' \in (t_{2k+1}, t_{2k+1} + t_\varepsilon) \tag{18}$$

$$\hat{G}_\alpha(t,t') = \hat{R}_2 = \begin{pmatrix} 1 & 0 \\ q & r \end{pmatrix} \qquad \text{for } t \in (t_{2k} - t_\varepsilon, t_{2k}),\ t' \in (t_{2k}, t_{2k} + t_\varepsilon). \tag{19}$$

For arbitrary t and t' the function $\hat{G}_\alpha(t,t')$ is easily found by taking into account the property of the $\hat{T}$ product:

$$\hat{G}_\alpha(t,t') = \hat{G}_\alpha(t,t'')\hat{G}_\alpha(t'',t') \qquad \text{for } t < t'' < t'. \tag{20}$$

So, for the function $\hat{G}_\alpha(t, t+T_{rf})$ appearing in equation (10) we have

$$\hat{G}_\alpha(t,t+T_{rf}) = \hat{G}_\alpha^{-1}(0,t)\hat{G}_\alpha(0,T_{rf})\hat{G}_\alpha(0,t) \qquad \text{for } t \in (0, T_{rf}/2) \tag{21}$$

where

$$\hat{G}_\alpha(0,T_{rf}) = \hat{G}_\alpha\left(0, \frac{T_{rf}}{2}\right)\hat{R}_1\hat{G}_\alpha\left(0, \frac{T_{rf}}{2}\right)\hat{R}_2. \tag{22}$$

Note that all the functions $\hat{G}_\alpha$ and their inverses which appear on the right of equations (21) and (22) are determined by equation (17). Thus, there are simple analytical expressions for the Green functions $\hat{G}_\alpha(t,t')$ for arbitrary time intervals in the OWLR model chosen here. Taking into consideration equations (16)–(22), the initial formula (10) can be transformed to

$$\varphi_\alpha(\omega) = \varphi'_\alpha(\omega) + \varphi'_{-\alpha}(\omega) \tag{23}$$

where

$$\varphi'_\alpha(\omega) = \frac{1}{\Gamma_0 T_{rf}}\langle W_1| \int_0^{T_{rf}/2} \mathrm{d}t\, \mathrm{e}^{-\mathrm{i}\tilde{\omega}t}\hat{G}_\alpha^{-1}(0,t)\frac{1}{\hat{1} - \mathrm{e}^{\mathrm{i}\tilde{\omega}T_{rf}}\hat{G}_\alpha(0,T_{rf})} \times \int_0^{t+T_{rf}} \mathrm{d}t'\, \mathrm{e}^{\mathrm{i}\tilde{\omega}t'}\hat{G}_\alpha(0,t')|1\rangle + \text{c.c.} \tag{24}$$

Then, equation (9) for the absorption cross-section takes the form

$$\sigma(\omega) = \frac{\sigma_a \Gamma_0^2}{2}\sum_\alpha |C_\alpha|^2 \varphi'_\alpha(\omega). \tag{25}$$

As seen from equation (24), the integrals over time are easily taken and, omitting the trivial details, we write down the final result in the analytical form

$$\varphi'_\alpha(\omega) = \frac{T_{rf}}{4(1+r)\Gamma_0}\left[\langle A_\alpha(\omega)|\frac{1}{\hat{1} - \mathrm{e}^{\mathrm{i}\tilde{\omega}T_{rf}}\hat{G}_\alpha(0,T_{rf})}|B_\alpha(\omega)\rangle - \Delta\tilde{\varphi}_\alpha\right] + \text{c.c.} \tag{26}$$

where

$$\hat{G}_\alpha(0, T_{rf}) = \begin{pmatrix} r\,\mathrm{e}^{-\mathrm{i}\omega_\alpha T_{rf}} + q^2 & qr \\ q\,\mathrm{e}^{-\mathrm{i}\omega_\alpha T_{rf}} & r\,\mathrm{e}^{-\mathrm{i}\omega_\alpha T_{rf}} \end{pmatrix} \tag{27}$$

$$\langle A_\alpha(\omega)| = (f(-\tilde{y} + y_\alpha), rf(-\tilde{y} - y_\alpha)) \tag{28}$$

$$|B_\alpha(\omega)\rangle = \left(\hat{1} + \mathrm{e}^{\mathrm{i}\tilde{y}}\hat{G}\left(0, \frac{T_{rf}}{2}\right)\hat{R}_1\right)\begin{pmatrix} f(\tilde{y} - y_\alpha) \\ f(\tilde{y} + y_\alpha) \end{pmatrix} \tag{29}$$

$$\Delta\tilde{\varphi}_\alpha(\omega) = \frac{1 - f(-\tilde{y} + y_\alpha)}{\mathrm{i}(\tilde{y} - y_\alpha)} + r\frac{1 - f(-\tilde{y} - y_\alpha)}{\mathrm{i}(\tilde{y} + y_\alpha)} \tag{30}$$

$$f(x) = \frac{\mathrm{e}^{\mathrm{i}x} - 1}{\mathrm{i}x} \tag{31}$$

$$\tilde{y} = \tilde{\omega}T_{rf}/2 \qquad y_\alpha = \omega_\alpha T_{rf}/2. \tag{32}$$

Using equations (25)–(32) the Mössbauer absorption spectrum under rf field excitation can be calculated for arbitrary frequency of the rf field, including both high and low frequency ranges, as well as for arbitrary values of the relaxation parameter q. Note that in the OWLR model considered here the transformation of the spectra with the rf field amplitude changing is simply determined by variations in the parameter q. It is obvious that this correlation can be rather diverse depending on the character of the relaxation processes, as well as on the geometric (the shape, volume and orientation of particles) and energy (positions of local minima and values of barriers) parameters.

Figure 3 shows examples of the transformation of the Mössbauer absorption spectra calculated within the OWLR model. In rf fields which are weak enough, when the relaxation effect can be neglected, i.e. for $q = 0$

$$|B_\alpha(\omega)\rangle = -\begin{pmatrix} [1 - \mathrm{e}^{\mathrm{i}(\tilde{y} - y_\alpha)}]/\mathrm{i}(\tilde{y} - y_\alpha) \\ [1 - \mathrm{e}^{\mathrm{i}(\tilde{y} - y_\alpha)}]/\mathrm{i}(\tilde{y} + y_\alpha) \end{pmatrix} \tag{33}$$

so that equation (26) is reduced to the form

$$\varphi'_\alpha(\omega) = -\frac{1}{2\Gamma_0}\mathrm{Im}\left(\frac{1}{\tilde{\omega} - \omega_\alpha} + \frac{1}{\tilde{\omega} + \omega_\alpha}\right) = \frac{1}{4}\left(\frac{1}{(\omega - \omega_\alpha)^2 + \Gamma_0^2/4} + \frac{1}{(\omega + \omega_\alpha)^2 + \Gamma_0^2/4}\right) \tag{34}$$

and the absorption spectrum is a superposition of Lorentzians with natural linewidth, which correspond to the static magnetic HF structure (see figure 3(a)).

In strong rf fields, when complete magnetization reversal occurs for half a period of the rf field, i.e. for $q = 1$, we easily find

$$\varphi'_\alpha(\omega) = \frac{T_{rf}}{4\Gamma_0}\left\{\frac{f(\tilde{y} - y_\alpha)[f(-\tilde{y} + y_\alpha) + f(\tilde{y} + y_\alpha)]}{1 - \exp(2\mathrm{i}\tilde{y})} + \frac{f(-\tilde{y} + y_\alpha)}{\mathrm{i}(\tilde{y} - y_\alpha)}\right\} + \text{c.c.} \tag{35}$$

which is the most compact representation of the well known result describing the collapse effect and formation of sidebands [7, 8] (see figure 3(e)).

4. Relaxation-stimulated resonances

The calculations performed for an intermediate range of the relaxation parameter, $0 < q < 1$, reveal a specific transformation of the spectral shape with changing rf field frequency. For most values of the rf field frequency, the behaviour shown in the central column of figure 3 takes place. With the relaxation rate q increasing or, identically, with the rf field amplitude increasing, a characteristic relaxation broadening of all spectral lines is observed, which is followed by the collapse of the magnetic HF structure into a single central line with sidebands.

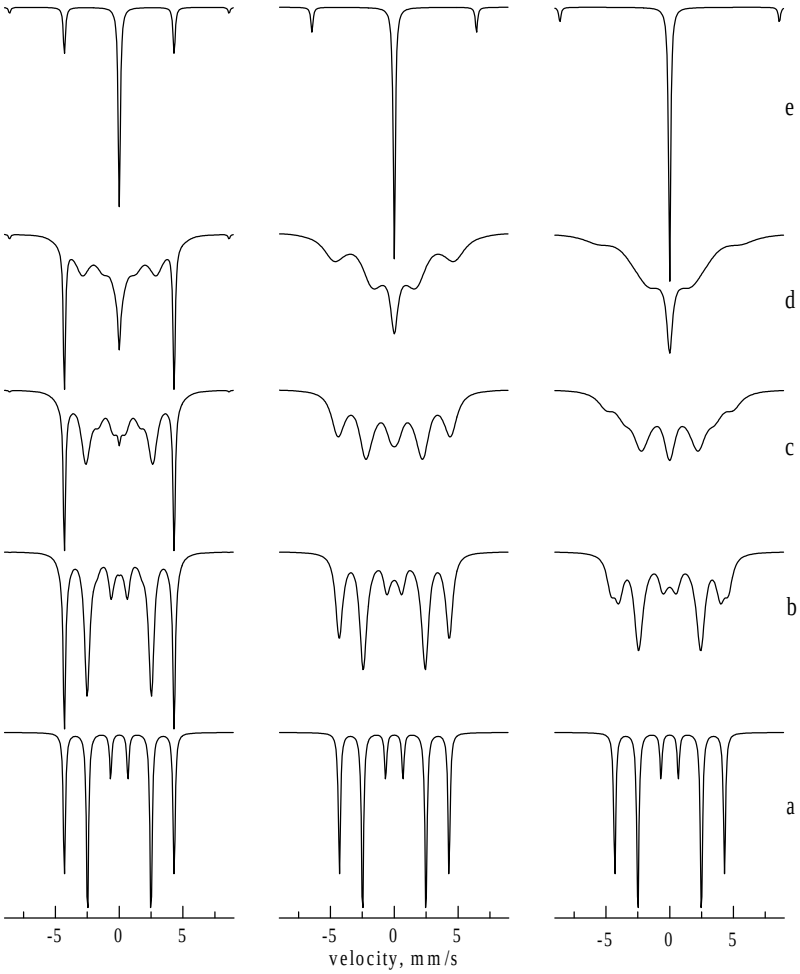

Figure 3. Transformation of the Mössbauer absorption spectra with the relaxation parameter $q = 0$, 0.2, 0.4, 0.6, 1 (a)–(e) of the OWLR model for different values of the rf field frequency $\omega_{rf}/2\pi = 50$ MHz (left column), 75 MHz (central column), and 100 MHz (right column). Here and below, the calculations are performed for the ^{57}Fe nuclei, $\omega_{3/2,1/2}/2\pi = 50$ MHz and a nonpolarized γ-beam transverse to the direction of an external rf field.

However, when the rf field frequency is equal to one of the magnetic HF structure frequencies or is related to the latter via the parametric resonance condition (1), a qualitatively different behaviour occurs. The left column in figure 3 corresponds to the resonant frequency

$$\omega_{rf} = \omega_{3/2,1/2} \equiv \tfrac{3}{2}\omega_e - \tfrac{1}{2}\omega_g. \tag{36}$$

As seen from this figure, in almost the whole range of q, where a well resolved HF structure is observed the outermost spectral lines hardly broaden and remain very narrow with the natural linewidth, whereas there is a substantial broadening of the inner spectral lines.

In the right column of figure 3, which corresponds to the resonant frequency

$$\omega_{rf} = 2\omega_{3/2.1/2} \tag{37}$$

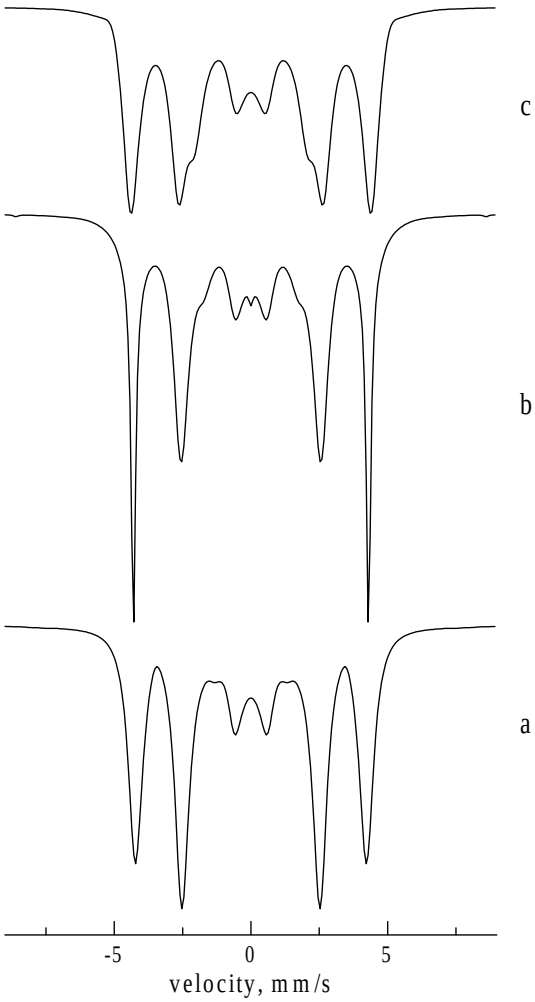

Figure 4. Mössbauer spectra calculated within the OWLR model at $q = 0.3$ in a rf magnetic field with the frequency $\omega_{rf}/2\pi = 45$, 50 and 55 MHz (a)–(c), near the frequency $\omega_{3/2,1/2}$.

a distinct splitting of the outermost spectral lines is observed at small values of q (figures 3(b) and (c)), while the inner spectral lines demonstrate a conventional relaxation broadening characteristic of the spectra in the central column of figure 3.

These results were actually obtained by analysing the shape of the Mössbauer spectra of magnetic systems, like an ensemble of the Stoner–Wohlfarth particles, by means of numerical calculations based on the general equations derived in [5, 8]. Obviously, it is impossible to understand the physical mechanisms of the formation of the resonant phenomena on the basis of general equations like equation (10), which not only has a simple analytical solution, but even requires a great deal of effort for its computer realization. The OWLR model helps one not only to derive rather simple equations for the description of the spectra, but also to express in a clear form the parameters of the spectral lines as a function of the relaxation parameter q and the rf field frequency in the vicinity of the resonances (1).

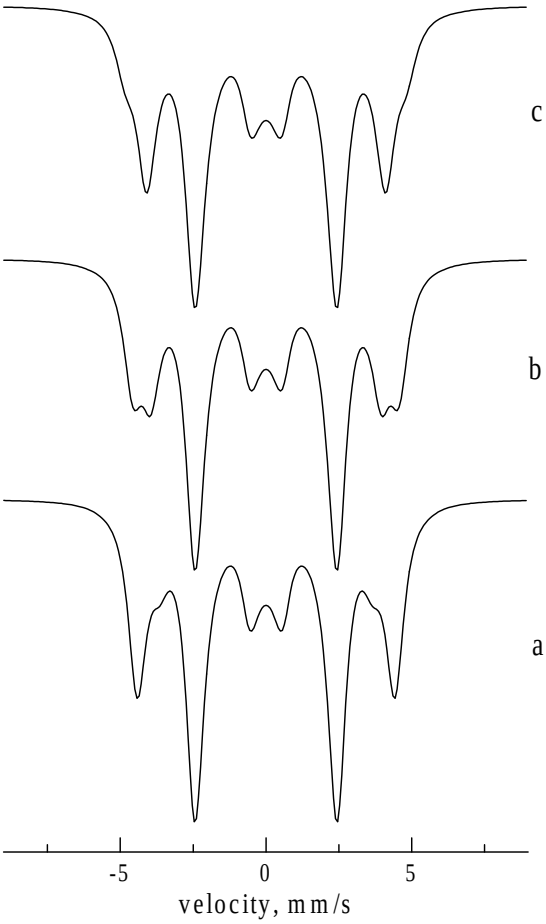

Figure 5. Mössbauer spectra calculated within the OWLR model at $q = 0.2$ in a rf magnetic field with the frequency $\omega_{rf}/2\pi = 94$, 99, and 104 MHz (a)–(c), near the doubled frequency $\omega_{3/2,1/2}$.

We will assume that the relaxation is slow enough, i.e.,

$$q \ll 1 \tag{38}$$

as well as considering spectral ranges in the vicinity of ω_α, so that

$$|\omega - \omega_\alpha| \ll \omega_\alpha. \tag{39}$$

The rf field frequency is considered to be close to one of the parametric resonance frequencies, i.e.,

$$|\omega_{rf} - \omega_\alpha^{(n)}| \ll \omega_\alpha \tag{40}$$

where

$$\omega_\alpha^{(n)} = \frac{2\omega_\alpha}{n}. \tag{41}$$

If conditions (38) and (39) hold, the vectors (29) and (30) do not depend on the frequency and they take the simplest forms

$$\langle A_\alpha(\omega) = (1\,0) \qquad |B_\alpha(\omega)\rangle = \begin{pmatrix} 1 \\ 0 \end{pmatrix}. \tag{42}$$

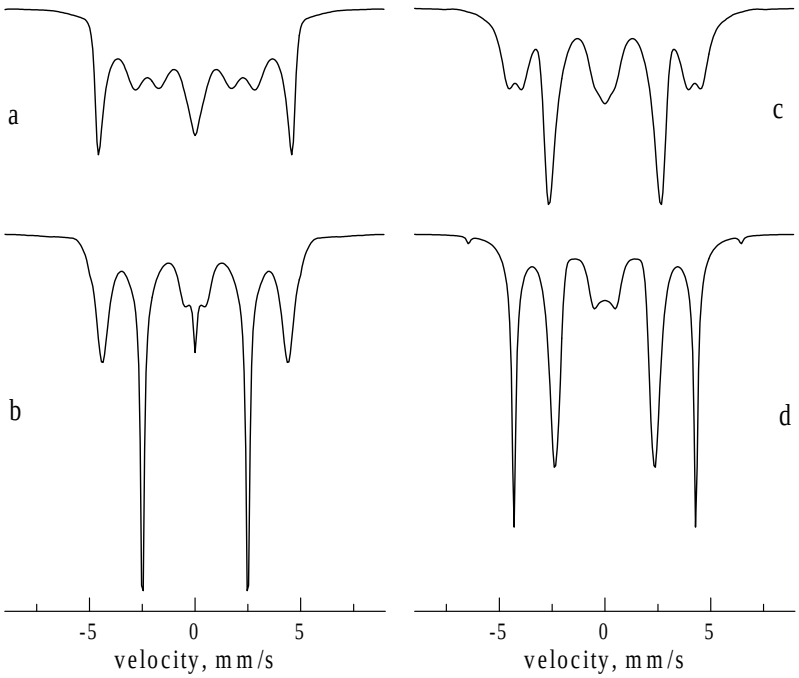

Figure 6. Mössbauer spectra calculated within the OWLR model at $q = 0.5$ in a rf magnetic field with the frequency $\omega_{rf}/2\pi = 54.5$ MHz near the doubled frequency $\omega_{1/2,1/2}$ (a), $\omega_{rf} = \omega_{1/2,1/2} = 2\pi \times 29$ MHz (b), $\omega_{rf} = 2\omega_{3/2,1/2}/3 = 2\pi \times 33$ MHz (c), $\omega_{rf} = \omega_{3/2,1/2}/2 = 2\pi \times 25$ MHz (d).

As far as the term (31) is concerned, it results in only a minor background correction to the first term in equation (26) and can be neglected. Moreover, in the framework of the approximation taken, one has to also neglect terms squared over q in equation (27) for the function $\hat{g}_\alpha$ (0, T_{rf}). As a result, equation (26) is reduced to a simpler form

$$\varphi_\alpha(\omega) = -\frac{1}{\Gamma_0}\mathrm{Im}\,\frac{\omega - \omega_\alpha - \Delta\omega + \mathrm{i}\Gamma/2}{(\omega - \omega_\alpha + \mathrm{i}\Gamma/2)(\omega - \omega_\alpha - \Delta\omega + \mathrm{i}\Gamma/2) \pm \gamma^2} \tag{43}$$

where

$$\gamma = \frac{q}{T_{rf}} \tag{44}$$

$$\Delta\omega = n\omega_{rf} - 2\omega_\alpha \tag{45}$$

$$\Gamma = \Gamma_0 + 2\gamma. \tag{46}$$

Signs (+) and (−) before the second term in the denominator of equation (43) correspond to the even and odd resonances (41). It is clear that equation (43) can be decomposed into two Lorentzians

$$\varphi_\alpha(\omega) = -\frac{1}{\Gamma_0}\mathrm{Im}\left(\frac{A_1}{\omega - \omega_\alpha - \lambda + \mathrm{i}\Gamma/2} + \frac{A_2}{\omega + \omega_\alpha - n\omega_{rf} + \lambda + \mathrm{i}\Gamma/2}\right) \tag{47}$$

where

$$\lambda = \tfrac{1}{2}(\sqrt{(\Delta\omega)^2 \mp 4\gamma^2} - |\Delta\omega|) \tag{48}$$

$$A_1 = \frac{|\Delta\omega| + \lambda}{|\Delta\omega| + 2\lambda} \qquad A_2 = \frac{\lambda}{|\Delta\omega| + 2\lambda}. \tag{49}$$

If the relaxation process is not essential and one can regard $\gamma = 0$, there is only the line at the position ω_α. As relaxation becomes involved, the second line appears at the position $(-\omega_\alpha + n\omega_{rf})$, i.e., at the place of the sideband from the hyperfine component at the position $-\omega_\alpha$. Thus, the relaxation process generates the appearance of sidebands.

From equations (48)–(49), such a generation is sharply resonant in character over the rf field frequency. In large detuning of ω_{rf} from the resonant frequency, $|\Delta\omega| \gg 2\gamma$, we have

$$A_1 = 1 - \frac{\gamma^2}{|\Delta\omega|^2} \qquad A_2 = \frac{\gamma^2}{|\Delta\omega|^2} \tag{50}$$

i.e., the intensity of the major line is close to unity and that of the sideband is rather small. On the other hand, in exact resonance, as seen from equations (48) and (49), the intensities of both the lines appear to be equal to each other,

$$A_1 = A_2 = 0.5. \tag{51}$$

It is also interesting to follow the transformation of the shapes of these two lines. There are two different kinds of behaviour depending on the parity of the resonance in this case. So, for the even resonance (see equation (36)), the value of λ in exact resonance appears to be purely imaginary so that both the lines coincide in their positions, but differ in width:

$$\Gamma_1 = \Gamma_0 \qquad \Gamma_2 = \Gamma_0 + 4\gamma. \tag{52}$$

When $\gamma \gg \Gamma_0$ the spectrum is a superposition of narrow and broad lines, which is revealed as a sharp increase in the peak intensity for these lines. This has been demonstrated by means of numerical calculations using the general equations (25)–(32) (see figure 4). With ω_{rf} detuning from the exact resonance, the width of the first line increases and that of the second line decreases so that at $|\Delta\omega| = 2\gamma$ they become equal and with $|\Delta\omega|$ increasing further the linewidths do not change.

A qualitatively different behaviour occurs for the odd resonance (see figure 5). In this case, the value of λ is always real and the widths of both the lines are equal to each other. However, on the other hand, as it is easily seen from equations (47) and (48), the lines cannot be in the same position in the spectrum, i.e., there is a minimum distance between them

$$\Delta_{12} = 2\gamma \tag{53}$$

and they cannot be closer to each other than this value.

The resonant effects described above reveal themselves not only for the outermost spectral lines, but also for the resonant frequencies (41) corresponding to the inner lines (see figures 6(a) and (b)), as well as for the resonant frequencies of higher orders n (see figures 6(c) and (d)).

Naturally, a question arises as to whether the effects predicted could be observed in real situations, for instance, when a sample consists of particles with random orientation of their easiest magnetization axes and the hyperfine field at the nucleus can smoothly change direction. Calculations performed using general equations like equation (10) show that for such systems, the characteristic features of the even resonances to a considerable extent remain as they are, whereas the odd resonances are essentially smoothed down. In order to observe the latter, textured samples need to be prepared.

5. Conclusions

The analysis carried out has allowed the peculiarities of the relaxation-stimulated resonance effects to be exposed in a distinct form. The proposed model of OWLR enables the Mössbauer absorption spectra under rf field excitation to be described in the simplest way. Using this model, the transformation of the spectra could be traced as a function of the rf field amplitude and frequency as well as the relaxation parameters.

Acknowledgment

We are grateful to the 'Internationales Büro des BMBF', Bonn, and the Russian Ministry of Science and Technology, Moscow, for supporting our collaboration on the project RUS-157-97.

References

[1] Pfeiffer L 1971 *J. Appl. Phys.* **42** 1725
[2] Hesse J *et al* 1998 *Hyperfine Interact.* **113** 499
[3] Matthias E 1968 *Hyperfine Interactions and Nuclear Transitions* ed E Matthias and D A Shirley (Amsterdam: North-Holland) p 815
[4] Vagizov F G, Manapov R A, Sadykov E K and Zakirov L L 1998 *Hyperfine Interact.* **116** 91
[5] Afanas'ev A M, Chuev M A and Hesse J 1997 *Phys. Rev.* B **56** 5489
[6] Stoner E C and Wohlfarth E P 1948 *Phil. Trans. Royal Soc. London* A **240** 599
[7] Julian S R and Daniels J M 1988 *Phys. Rev.* B **38** 4394
[8] Afanas'ev A M, Chuev M A and Hesse J 1998 *JETP* **86** 983